



In situ FT-IR spectroscopic investigations of species from biomass fuels in a laboratory-scale combustor: the release of nitrogenous species

A. Weissinger, T. Fleckl, and I. Obernberger*

Institute for Ressource Efficient and Sustainable Systems, Thermal Biomass Utilisation, Graz University of Technology, Inffeldgasse 25, 8010 Graz, Austria

Received 1 July 2002; received in revised form 13 February 2004; accepted 27 February 2004

Available online 9 April 2004

Abstract

In situ FT-IR absorption spectroscopy was used with a laboratory-scale reactor and thermogravimetric analysis to describe the release of nitrogen-containing compounds from a fixed bed of fibreboard residues. Such in situ detection of NH_3 requires knowledge of the absorption coefficients at high temperatures. These coefficients were obtained from calibrations using a laboratory-scale reactor at temperatures up to 800°C , as well as from calculations using a database. On the basis of laboratory experiments, the rates of release of N species, of the major C species (CO , CO_2 , and CH_4), and of H_2O have been derived. It is concluded that the release of nitrogen from the fuel can be modelled if such parameters as the superficial velocity and the flow rate of oxygen are known. This method allows profiles of the nitrogenous species to be generated and used as input data for CFD calculations based on thermodynamic combustion models for a fixed bed on a grate.

© 2004 The Combustion Institute. Published by Elsevier Inc. All rights reserved.

Keywords: Biomass; Fixed bed combustion; FT-IR spectroscopy; NO_x formation

1. Introduction

In addition to emissions of particles, NO_x constitutes a major research topic in biomass combustion. Reliable boundary conditions concerning the inlet concentrations of NO_x precursors (HCN , NH_3) and NO_x species (NO , NO_2 , N_2O) are necessary for optimising NO_x reduction when burning biomass on grate furnaces. It is of special importance in the case of grate furnaces to obtain a time-resolved function, which describes the release of the species along a grate. This work evaluates a methodological approach

combining experimental test runs and theoretical kinetic models of combustion in a fixed bed combustion. It is common to describe combustion on a grate by a model of a downwards propagating reaction front in a fixed bed. Various approaches have been applied for coal and biomass fuels, such as wood chips and straw [1–4]. So far all these investigations and the models describing a fuel's conversion have focused on the release of C, but not on N species, because the related NO_x chemistry would result in an immense computational effort.

By means of test runs, the release of NO_x and their precursors (HCN , NH_3) from a fixed bed was investigated in relation to combustion-specific parameters by FT-IR in situ absorption measurements and extractive measurements using a heated suction probe.

* Corresponding author. Fax: +43-(0)-316-481300-4.
E-mail address: obernberger@rns.tugraz.at
(I. Obernberger).

These N species form the major potential for forming fuel- NO_x and are therefore referred to as TFN (total fixed nitrogen). Under specific combustion conditions and in the presence of NO, both HCN and NH_3 can be reduced to N_2 , instead of being oxidised to NO_x . Optimisation measures to achieve these combustion conditions are called primary measures for NO_x reduction [5]. The motivation of this work was to investigate possible links between such theoretical combustion models with empirical models for the release of nitrogen, based on experiments. These representative profiles for the release of nitrogen along a grate can be used for kinetic studies and CFD simulations. An improvement of the theoretical investigation of primary measures for reducing NO_x from fixed bed combustors of biomass will thus be achieved in the future.

2. Principles of in situ FT-IR spectroscopy

Fourier transform infrared (FT-IR) in situ absorption spectroscopy is a useful technique for investigating flue gas components in various combustion systems. The advantage of this technique over conventional extractive method is that the hot gases do not need to be cooled and filtered before performing measurements. Because of this, possible changes of the gas composition due to the temperature dependence of chemical equilibria can be avoided. The application of an FT-IR spectrometer to in situ gas quantification requires knowledge of the absorption coefficients of the relevant gases at high temperatures. These coefficients may be obtained either experimentally or theoretically using molecular data. Previously [6,7] the absorption coefficients of CO , CO_2 , CH_4 , and H_2O have been determined for measurements in a grate furnace fuelled with biomass (nominal boiler load 440 kW_{th}). This paper applies FT-IR spectroscopy to a laboratory-scale reactor focusing on the release of nitrogen compounds from the bed of fuel. The major detectable species containing nitrogen was expected to be NH_3 . Because NH_3 had not been detected with the experimental set-up used formerly [6], a specially modified experimental arrangement was used and tested for the calibrations and measurements of $[\text{NH}_3]$. Furthermore, the present paper compares experimental spectra of NH_3 with those from the HITRAN (high transmission) molecular absorption database [8]. In addition, the results obtained below are verified by means of elemental balances. The methodology of the signal processing and calculation of the concentrations have been published previously [7].

3. Experimental

3.1. Experimental set-up and methodology

The laboratory-scale combustor was a discontinuously operated pot furnace. It consisted of a cylindrical retort (height 0.35 m, i.d. 0.12 m), heated electrically by two separated PID controlled-heating circuits. The fuel was put into a cylindrical holder (0.100 m height and 0.095 m i.d.). Both parts were made of fibre-reinforced SiC ceramics to avoid CO , NO , and ash reacting with the wall. The sample holder was mounted on a plate, which was put on a balance to investigate the mass loss during fuel oxidation (Sartorius GP 4001, ± 0.1 g) and placed into the upper position as shown in Fig. 1a with the dotted lines. Air or a mixture of $\text{O}_2 + \text{N}_2$ was introduced through a porous plate at the bottom of the fuel bed. A liquid sealing filled with thermal oil (Therminol 66) was used to separate the balance and the reactor mechanically and to keep the surrounding air from entering the reaction zone as a bypass stream above the fuel bed. Species concentrations in the flue gas directly above the fuel bed were measured with in situ FT-IR absorption spectroscopy. For the measurement of $[\text{NH}_3]$, ZnSe windows were mounted on a stainless steel flange, located on the retort outside the heated part (Fig. 2). In this case the path length was influenced by the nitrogen purging the flanges; this prevented hot gases from entering the flanges and kept the windows cool (see calibration section). Additionally, a mounting for a sapphire window could be put into the optical path directly in the hot region. Sapphire windows have the advantage of withstanding high temperatures (unlike ZnSe), so that the path length in the absorbing gas was determined only by the distance between the windows (0.12 m), because no purging was necessary. The disadvantage of sapphire windows is that the detection of NH_3 is not possible because of their optical properties (opaque at a spectral region < 1900 cm^{-1}). A Midac M2401-C spectrometer with a maximum resolution of 0.5 cm^{-1} equipped with a nitrogen-cooled MCT detector was used for all the experiments. The velocity of the moving mirror of the spectrometer was set to 5.1 cm/s. Triangular apodisation, the Mertz method for phase correction, and $4 \times$ zero-filling were used to obtain a spectrum. For each spectrum investigated 20 scans were averaged. The data collection time was ~ 16.7 s per spectrum. A detailed description of the FT-IR in situ absorption spectroscopy applied is available [6].

In addition, the concentrations of NO, HCN, and NH_3 were determined by extracting a gaseous sample using a heated suction probe. Chemiluminescence detection (CLD) was applied for NO and NO_2 using

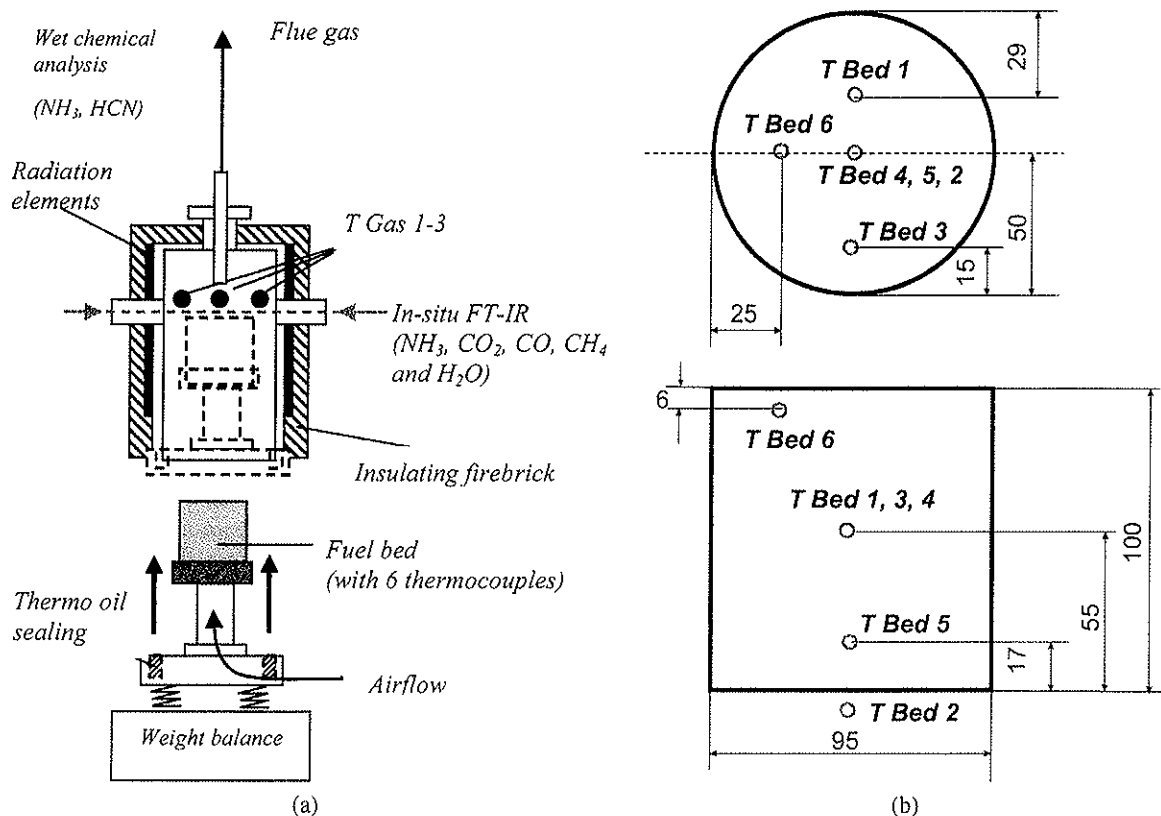


Fig. 1. Schematic experimental set-up (a) and arrangement of the thermocouples in the fuel bed (b).

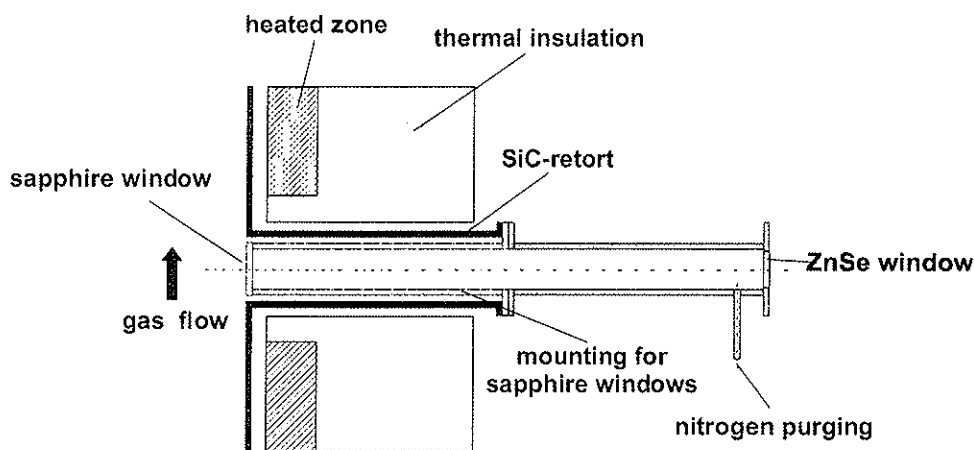


Fig. 2. Schematic arrangement of the windows for FT-IR spectroscopy.

an ECO Physics 740 ht. Wet chemical analysis was used for HCN and NH_3 with a colourimetric method (HCN, Method 4500-CN-E. Colorimetric Method 4-39; and NH_3 , Method 4500-NH₃-F. Phenate Method 4-108 from [9]). The flue gas was diluted 1/10 with N_2 (DEKATI DILUTER) before it entered the ECO Physics equipment to avoid hazardous concentrations of CO, which might destroy the apparatus. [NH_3] and [HCN] were measured directly without dilution of the flue gas.

Thermocouples ($T_{\text{Bed 1}}$ to $T_{\text{Bed 6}}$) were placed in the sample holder of the fuel bed to follow the propagation of the reaction front by measuring the time-dependent temperature distribution in the bed of fuel. Five thermocouples were placed in the bed according to Fig. 1b. Thermocouple $T_{\text{Bed 2}}$ was placed on the axis of the combustor, directly beneath the bed to measure the temperature of the combustion air. The experimental conditions were derived from experience with grate furnaces [11].

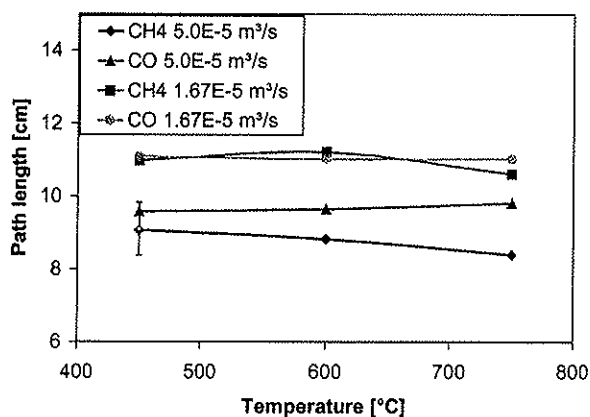


Fig. 3. Path length as a function of the temperature at different purging rates (1.67×10^{-5} and $5.0 \times 10^{-5} \text{ m}^3/\text{s}$). The concentrations used were 20 vol% of CO and 5 vol% of CH₄ in N₂ at a flow rate of $3.0 \times 10^{-4} \text{ m}^3/\text{s}$.

3.2. Calibration of the NH₃ measurement by in situ FT-IR spectroscopy

The performance of measurements using ZnSe windows and nitrogen-purging requires knowledge about the influence of purging on the path length in the absorbing gas. This was investigated experimentally using defined concentrations of CO and CH₄ at different temperatures, purging, and gas flow rates. Absorbance spectra of CO and CH₄ had already been recorded in previous experiments in a high-temperature calibration cell equipped with sapphire windows at a defined path length l_{cal} [7]. Comparing the spectra recorded in the laboratory-scale reactor $A_{\text{eff}}(\nu)$ with the spectra recorded in the high-temperature gas cell $A_{\text{cal}}(\nu)$ using the same concentrations results in an effective path length l_{eff} at defined flow conditions according to

$$l_{\text{eff}} = l_{\text{cal}} \cdot \frac{A_{\text{cal}}(\nu_0)}{A_{\text{eff}}(\nu_0)} \quad [\text{cm}]. \quad (1)$$

The experimental set-up was slightly modified for calibration. The fuel bed was filled with a layer of ZrO spheres (diam. 2 mm) to obtain uniform flow conditions. The calibration gases were passed through the layer using the combustion air port. Flow rates were varied between 3×10^{-4} and $9.67 \times 10^{-4} \text{ m}^3/\text{s}$ using a mass flow controller (Tylan Series 2920).

The path length was shown to have a small dependence on temperature (see Fig. 3). A difference of nearly 15% between the path lengths for CO and CH₄ can be observed at 750 °C and a nitrogen purging rate of $5 \times 10^{-5} \text{ m}^3/\text{s}$. The major influence on the path length results from the rate of purge gas flow (Fig. 4). At a high flow rate and a purging rate of $1.67 \text{ m}^3/\text{s}$ the path length was longer than the diameter of the retort (0.12 m), indicating that small amounts of the calibration gases had entered the flange. A trend to

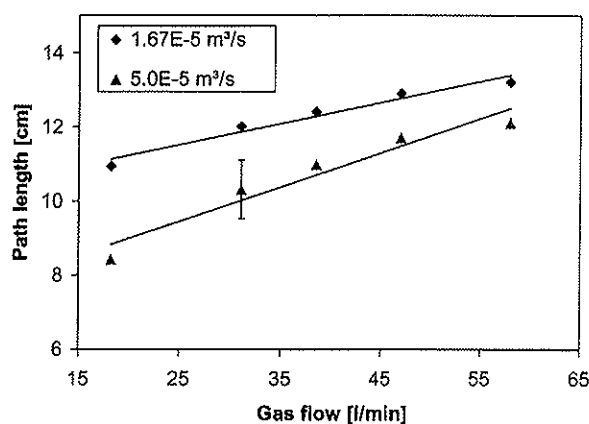


Fig. 4. Path length as a function of gas flow at different purging rates. Experiment carried out at a concentration of 5 vol% CH₄ in N₂ at a temperature of 700 °C. Nitrogen purging rates of the flanges were 1.67×10^{-5} and $5.0 \times 10^{-5} \text{ m}^3/\text{s}$.

a maximum path length at higher flow rates was observed. A purging rate of $5 \times 10^{-5} \text{ m}^3/\text{s}$ was thus chosen for all combustion experiments. The error in the effective path lengths was estimated to be $\pm 10\%$. Experiments investigating the influence of H₂O and CO₂ on the path length were not performed. It was assumed that the relations observed for CO and CH₄ regarding the effective path length are also valid for other species. The path length was regarded as being independent of temperature and other species in all the experiments performed. A verification of these assumptions has been made during the combustion experiments by comparison with test runs using sapphire windows as a reference (see Figs. 7–12).

Calibration spectra for NH₃ were recorded for temperatures between 300 and 800 °C. The experiments were performed with a gas flow of NH₃ of $3 \times 10^{-4} \text{ m}^3/\text{s}$ and a purging rate of $1.67 \times 10^{-5} \text{ m}^3/\text{s}$, which corresponds to a path length of 0.109 cm for the flow rate of the calibration gas (Fig. 4). A gas divider (MGV-25 LN Industries SA) was used to obtain [NH₃] between 2880 and 11,520 vppm. Spectra of NH₃ were calculated for the same concentrations and temperatures using a resolution of $0.6 \text{ cm}^{-1} \pm 10\%$ for all calculations [7]. Fig. 5 compares the measured and calculated spectra of NH₃; in fact, they show a good qualitative correspondence. Deviations between the measured and calculated spectra can be found in the spectral region between 935 and 955 cm^{-1} . Absorbance values of the relevant spectral sections are given for two different temperatures (300 and 800 °C) and for two different concentrations (Table 1). The spectral regions investigated for each gaseous species were chosen to ensure that any overlapping with bands from the other flue gas compounds (CO₂ and H₂O) was reduced to a minimum and had only a minor influence. The errors in absorbance for the cal-

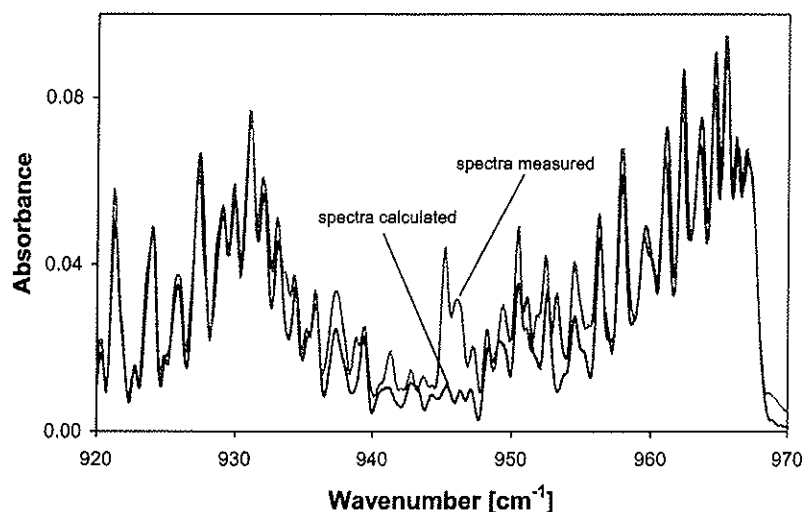


Fig. 5. Measured and calculated absorbance of NH_3 as function of wavenumber. Spectra measured and calculated at a concentration of 11,520 ppm NH_3 , a temperature of 800 °C, and a path length of 10.9 cm.

Table 1

Measured and calculated absorbance of the relevant spectral sections for NH_3 during calibration at different NH_3 concentrations in the calibration gas

Spectral section (cm^{-1})	Temperature (°C)	Measured absorbance 2880 ppm	Calculated absorbance 2880 ppm	Measured absorbance 11520 ppm	Calculated absorbance 11520 ppm
924.0	300	0.020 ± 0.005	0.023 ± 0.005	0.082 ± 0.014	0.086 ± 0.017
957.9	300	0.020 ± 0.005	0.021 ± 0.004	0.082 ± 0.014	0.081 ± 0.016
966.1	300	0.065 ± 0.012	0.060 ± 0.012	0.249 ± 0.039	0.227 ± 0.045
1122.2	300	0.079 ± 0.014	0.080 ± 0.016	0.252 ± 0.040	0.235 ± 0.047
1159.0	300	0.060 ± 0.011	0.062 ± 0.012	0.230 ± 0.037	0.220 ± 0.044
924.0	800	0.014 ± 0.004	0.012 ± 0.002	0.048 ± 0.009	0.047 ± 0.009
957.9	800	0.019 ± 0.005	0.016 ± 0.003	0.067 ± 0.012	0.061 ± 0.012
966.1	800	0.020 ± 0.005	0.017 ± 0.003	0.070 ± 0.013	0.068 ± 0.014
1122.2	800	0.031 ± 0.007	0.035 ± 0.007	0.120 ± 0.020	0.116 ± 0.023
1159.0	800	0.031 ± 0.007	0.036 ± 0.007	0.120 ± 0.020	0.133 ± 0.027

culated spectra were derived from the errors of the spectral data and the resolution determined and estimated to be $\pm 20\%$ at least. Errors in the measured spectra were estimated from the error of the spectrometer adjustment ($\pm 5\%$), from a statistical error of ± 0.002 absorption unit, and from the error of the path length ($\pm 10\%$). Considering the errors of the measured and calculated absorbance, satisfactory quantitative correspondence can be reported for the ranges of concentration and temperature investigated.

3.3. Calculation of the combustion specific parameters and the mass balances for plausibility control

3.3.1. Parameters characteristic of fixed bed combustion

The time-independent parameters, which were varied during the test runs, included the superficial velocity at the inlet (SV_{inlet}), determined by the flow rate of the combustion air (V_{inlet}), and $[\text{O}_2]$ in the in-

let gas stream ($y_{\text{O}_2_{\text{inlet}}}$). These two parameters were kept constant during a test run and may be correlated with the overall rates of conversion during the whole test run, or during a specific time interval, e.g., the phase of combined drying and gasification. These parameters are useful if the gas concentrations and the release of certain species remained constant for the investigated time interval, as was expected for the propagation time of the reaction front. SV_{inlet} was calculated from the combustion air flow and the cross sectional area of the fuel bed (A):

$$SV_{\text{inlet}} = V_{\text{inlet}}/A \text{ [m/s].} \quad (2)$$

The molar flow rate of O_2 ($r_{\text{O}_2_{\text{inlet}}}$) into the reactor and the fuel bed can be calculated using the molar volume (V_m):

$$r_{\text{O}_2_{\text{inlet}}} = V_{\text{inlet}}(y_{\text{O}_2_{\text{inlet}}}/V_m) \text{ [mol/s].} \quad (3)$$

The propagation velocity (u_{RF}) of the reaction front depends on the combustion conditions. It was calculated for each test run as the mean value of the

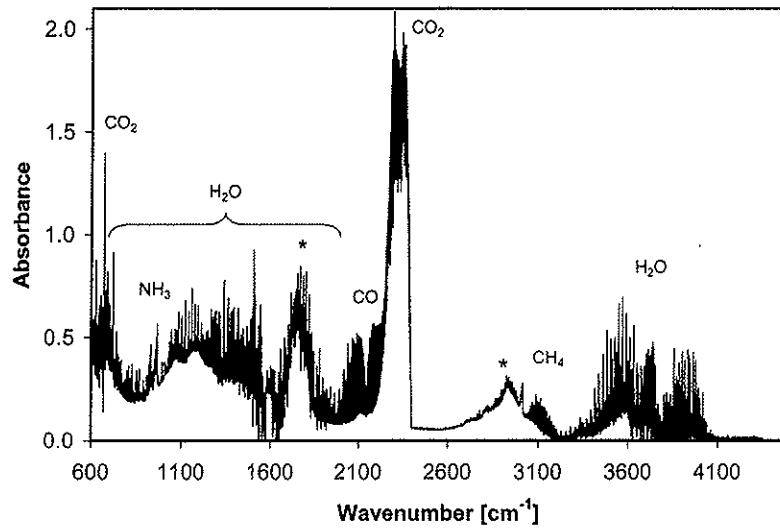


Fig. 6. Absorbance as a function of wavenumber. Spectrum recorded after a duration of 500 s. The air flow was set to $6.67 \text{ m}^3/\text{s}$; the asterisk (*) indicates a region of not clearly identified species. In comparison with spectral tables at ambient temperature as reference, these spectral lines may be explained as bands of higher hydrocarbons.

time shift measured at 200, 400, and 600 °C and the distance between the top and bottom thermocouple ($d_{T_{\text{Bed}6}-T_{\text{Bed}5}}$) in the fuel bed ($T_{\text{Bed}6}$ and $T_{\text{Bed}5}$). This means that u_{RF} is a constant parameter for each test run and can be compared with the integrated released amount of N:

$$u_{\text{RF}} = d_{T_{\text{Bed}6}-T_{\text{Bed}5}} / \Delta t_{\text{T}} \text{ [m/s]}. \quad (4)$$

To describe of the release of nitrogenous species along a grate, parameters that show a time-dependent behaviour as a result of the combustion conditions achieved in the bed must be investigated. Possible parameters for investigation include the superficial velocity of the combustion gases at the outlet of the bed (SV_{outlet}),

$$SV_{\text{outlet}} = V_{\text{Gas}} / A \text{ [m/s]}, \quad (5)$$

the stoichiometric ratio (air/fuel ratio; SR) in the bed, and the normalised mass loss $m/m_{\text{fuel_init}}$ as a function of the initial mass of the sample ($m_{\text{fuel_init}}$) and the mass of the sample at a certain time ($m_{\text{fuel}(t)}$):

$$m/m_{\text{fuel_init}} = \frac{m_{\text{fuel_init}} - m_{\text{fuel}(t)}}{m_{\text{fuel_init}}}. \quad (6)$$

3.3.2. Control of FT-IR in situ measurements

Three-dimensional functions connecting concentration, temperature, and absorbance at selected spectral regions were used to determine the concentrations of flue gas components [6]. These functions were fitted to the measurements of [CO], [H₂O], [CO₂], and [CH₄] in a high-temperature calibration cell [7], as well as to the data gained from the NH₃ calibration. With these functions it was possible to obtain the species concentrations at a given temperature and

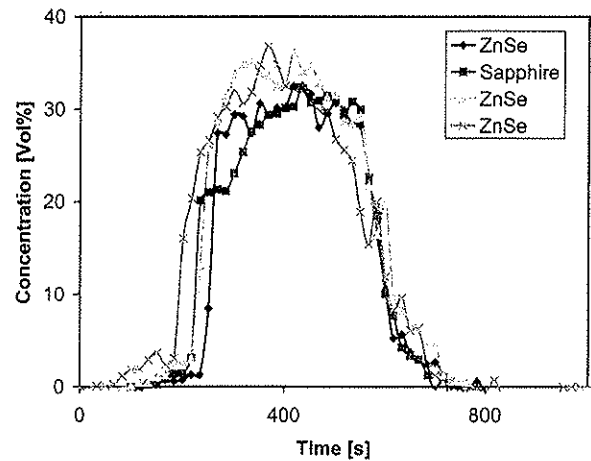


Fig. 7. Concentrations of H₂O as a function of time at an air flow rate of $6.67 \text{ m}^3/\text{s}$.

absorbance. The temperature was measured by a thermocouple mounted on the axis of the retort at the height at which the beam passed to the spectrometer (see Fig. 1a). A typical spectrum recorded during a test run is shown in Fig. 6. Spectral regions of identified species are marked with their names, while regions of unknown species are marked with an asterisk (*). With reference to spectral tables at ambient temperature, these spectral lines may be explained as bands of higher hydrocarbons. For a more detailed interpretation, spectra of the expected components must be recorded at the relevant temperatures.

Figs. 7–12 show the concentrations of [H₂O], [CO], [CO₂], [CH₄], and [NH₃] as functions of time during test runs with an air flow rate of $6.67 \times 10^{-4} \text{ m}^3/\text{s}$. It can be seen that the [H₂O] and [CO₂] determined during the test run using sapphire windows were in the range of fluctuations of the test

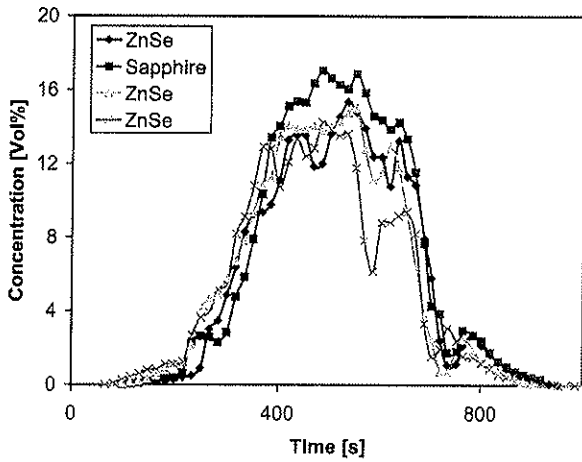


Fig. 8. Concentrations of CO as a function of time at an air flow rate of 6.67 m³/s.

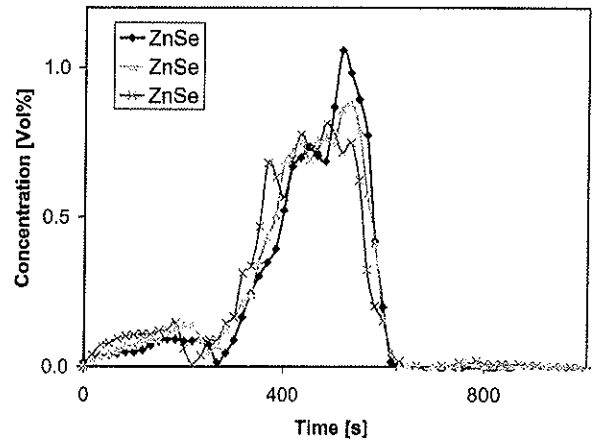


Fig. 11. Concentrations of NH₃ as a function of time at an air flow rate of 6.67 m³/s.

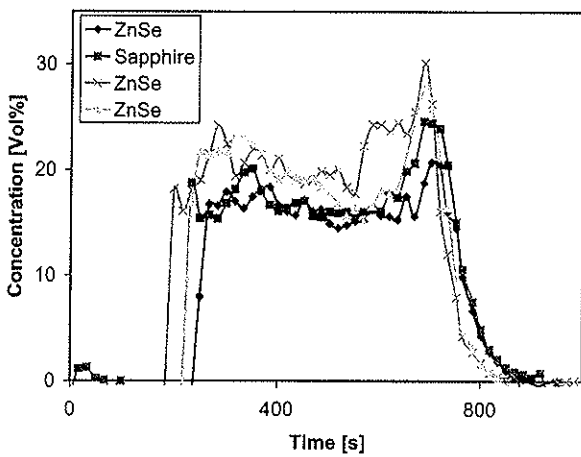


Fig. 9. Concentrations of CO₂ as a function of time at an air flow rate of 6.67 m³/s.

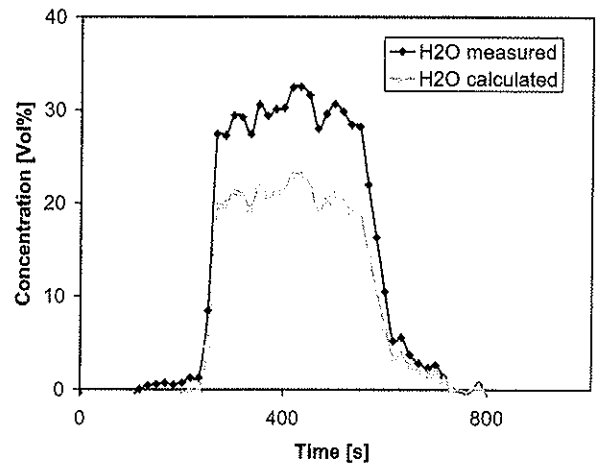


Fig. 12. Concentrations of H₂O as a function of time at an air flow rate of 6.67 m³/s. Determination of the concentration was based on calibration functions measured (H₂O measured) and calculated (H₂O calculated).

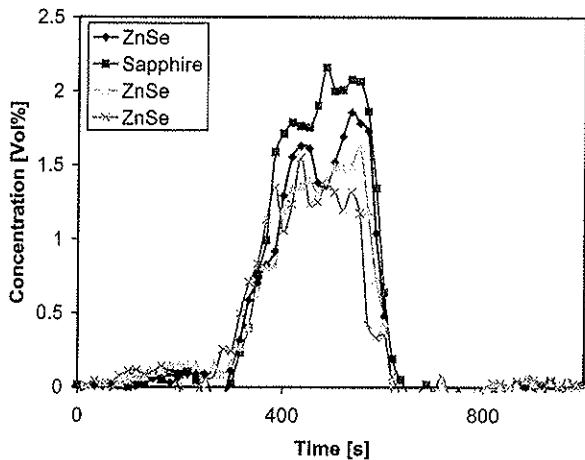


Fig. 10. Concentrations of CH₄ as a function of time at an air flow rate of 6.67 m³/s.

runs using ZnSe windows. Concentrations of CO and CH₄ were slightly higher using sapphire windows. The total error of the purging arrangement was estimated to be ±15–20% (based on the assumption of

a constant flow rate of gas during the experiments and the error of the path length (±10%). Considering this, the concentrations obtained with and without sapphire windows showed satisfactory agreement. Hence, the assumptions made and the experimental set-up used seemed to be meaningful. Leakage of substantial amounts of hot gases into the flanges could also be excluded, because cold layers in the line of sight would result in a strong decrease of the concentration of CO and CH₄ due to their higher absorbance at lower temperatures, which could not be detected [6]. The plausibility of the measured concentrations was tested by calculating mass and elemental balances for the components H, C, and N. Because composition of the fibreboard fuel used (Table 4) and weight of the fuel were known it was possible to calculate an integral released amount of each element based on either the recorded mass loss or the gas concentrations determined by the FT-IR measurements. By neglecting O₂, H₂, and hydrocarbons

(except CH₄), the mole fraction of molecular nitrogen y_{N_2} was calculated by subtracting the sum of the mole fractions measured by the FT-IR spectrometer, y_i ($i = \text{CO, CO}_2, \text{H}_2\text{O, CH}_4, \text{NH}_3$), from 1:

$$y_{N_2} = 1 - \sum y_i \text{ [mol/mol]}. \quad (7)$$

The total flow rate of nitrogen entering the retort (V_{in}) is defined according to the experimental conditions (Table 2). The flow rate of product gas in the retort at normal conditions can thus be calculated as

$$V_{gas} = V_{in}/y_{N_2} \text{ [m}^3\text{/s]}. \quad (8)$$

Each measured y_i can be converted to a concentration [mol/l] using the molar volume under normal conditions V_m :

$$c_i = y_i / V_m \text{ [mol/m}^3\text{]}. \quad (9)$$

In fact, c_i and V_{Gas} were used to obtain an instantaneous release rate of a species r_i :

$$r_i = c_i \cdot V_{gas} \text{ [mol/s]}. \quad (10)$$

The release rate of each chemical element (C, N or H) is

$$r_H = 2r_{H_2O} + 3r_{NH_3} + 4r_{CH_4} \text{ [mol/s]}. \quad (11)$$

$$r_C = r_{CO} + r_{CO_2} + r_{CH_4} \text{ [mol/s]}. \quad (12)$$

$$r_N = r_{NH_3} \text{ [mol/s]}. \quad (13)$$

The overall amount released during a test run can be obtained for each element by summation of the instantaneous release rates and was normalised with the overall amount released for each element, calculated from the mass loss and the original elemental composition. A zero value means that the element was not measured with the FT-IR system; a value of 1 means that the entire initial amount of the element was measurable after conversion. Values >1 are not physically meaningful. Since the determination of [H₂O] has higher uncertainties than that of the other components [6,7], two separate balances were made based on [H₂O] obtained from calculated and measured calibration functions. Both concentrations are shown in Fig. 12 as a function of time. The values for [H₂O] obtained from the calculated functions are 25% lower than the values based on the measured functions. This difference has a big influence on the balances. A higher [H₂O] results in an increased product gas flow (Eqs. (7) to (13)) and therefore in higher release rates.

The results of the elemental balances calculated are shown in Tables 2 and 3. The errors given were

Table 2

Balances of H, C, and N using H₂O concentrations obtained by calculated calibration functions

Window	Air flow rate (m ³ /s)	H-balance (mol/mol _{fuel})	C-balance (mol/mol _{fuel})	N-balance (mol/mol _{fuel})
ZnSe	3.33 × 10 ⁻⁴	0.70 ± 0.21	0.83 ± 0.17	0.40 ± 0.08
ZnSe	3.33 × 10 ⁻⁴	0.86 ± 0.26	1.07 ± 0.21	0.37 ± 0.07
Sapphire	3.33 × 10 ⁻⁴	0.82 ± 0.21	1.12 ± 0.17	–
ZnSe	6.67 × 10 ⁻⁴	0.71 ± 0.21	0.86 ± 0.17	0.25 ± 0.05
ZnSe	6.67 × 10 ⁻⁴	1.00 ± 0.30	1.13 ± 0.23	0.31 ± 0.06
ZnSe	6.67 × 10 ⁻⁴	0.91 ± 0.27	1.18 ± 0.24	0.28 ± 0.06
Sapphire	6.67 × 10 ⁻⁴	0.68 ± 0.17	0.97 ± 0.15	–
Mean value	3.33 × 10 ⁻⁴	0.79 ± 0.08	1.01 ± 0.16	0.39 ± 0.02
Mean value	6.67 × 10 ⁻⁴	0.83 ± 0.16	1.04 ± 0.15	0.28 ± 0.03

Table 3

Balances of H, C, and N using H₂O concentrations obtained by measured calibration functions

Window	Air flow rate (m ³ /s)	H-balance (mol/mol _{fuel})	C-balance (mol/mol _{fuel})	N-balance (mol/mol _{fuel})
ZnSe	3.33 × 10 ⁻⁴	1.54 ± 0.77	1.16 ± 0.46	0.60 ± 0.24
ZnSe	3.33 × 10 ⁻⁴	1.89 ± 0.95	1.50 ± 0.60	0.56 ± 0.22
Sapphire	3.33 × 10 ⁻⁴	1.80 ± 0.63	1.57 ± 0.39	–
ZnSe	6.67 × 10 ⁻⁴	1.56 ± 0.78	1.20 ± 0.48	0.38 ± 0.15
ZnSe	6.67 × 10 ⁻⁴	2.20 ± 1.10	1.58 ± 0.63	0.47 ± 0.19
ZnSe	6.67 × 10 ⁻⁴	2.00 ± 1.00	1.65 ± 0.66	0.42 ± 0.17
Sapphire	6.67 × 10 ⁻⁴	1.50 ± 0.52	1.36 ± 0.34	–
Mean value	3.33 × 10 ⁻⁴	1.75 ± 0.18	1.41 ± 0.22	0.58 ± 0.03
Mean value	6.67 × 10 ⁻⁴	1.82 ± 0.34	1.45 ± 0.21	0.42 ± 0.05

estimated from the errors of the FT-IR measurements [7]. It can be seen that the H and C balances show plausible results for $[H_2O]$ obtained by calculated calibration functions. In contrast, $[H_2O]$ obtained by measured functions, produced values > 1 for the overall amount of H released, which is not possible. Considering the errors of the mean values of the H and the C balances, no significant differences can be observed between the two test series. Only the N balance shows a significant difference. The differences between 1 (total recovery) and the calculated released amount of each element (Table 2) can be interpreted as species that cannot be quantified by FT-IR in situ measurements, such as N_2 , NO, and HCN for N species and hydrocarbons (except CH_4) for C species.

4. Experimental results of the laboratory-scale reactor test runs

Tests were performed using fibreboard residues as fuel (for composition see Table 4). The flow rates and O_2 concentrations in the inlet gas stream were set for typical operating conditions of a grate furnace with flue gas recirculation under the grate. These operating conditions were obtained during experiments performed with a horizontally moving grate furnace and have been described previously [10,11]. In total 8 different inlet conditions were investigated, and each inlet condition was investigated at least in triplicate. A detailed description of the parameters during the test runs can be seen in Table 5. Experiments were started by introducing the sample holder of the fuel

bed into the preheated retort ($750^\circ C$). Due to radiation, the sample was ignited at the top. A downward propagating reaction front could be observed during drying and devolatilisation. When the reaction front reaches the bottom of the fuel bed, this phase ends and heterogeneous char burnout starts. Ignition was identified by a peak in the gas temperatures ($T_{Gas\ 1-3}$) and thermocouple T_{Bed6} , located directly beneath the upper surface of the fuel bed (Fig. 1). The starting time for char burnout was defined as the time when thermocouple T_{Bed5} , located at the bottom of the fuel bed, showed the highest temperature of all the thermocouples in the pot furnace (see Figs. 1 and 14).

The loss of mass by the fuel sample was determined by weighing and by the concentrations of the relevant species CO, CO_2 , H_2O , and NH_3 , which were measured directly above the bed by FT-IR spectroscopy. The two combustion phases showed significantly different releases of N species. During each combustion phase, the concentration of each gas remained almost constant (see Figs. 7–12). Thus each gas species had a constant concentration during devolatilisation; this supports the notion of combined drying and devolatilisation in a reaction front and a constant rate of release during the propagation of the reaction front. In general, reproducibility was satisfactory. The temperature profile in the fuel and the release of mass as a function of time particularly showed satisfactory reproducibility (see Figs. 13 and 14). Only the release of NO showed stronger variations [11]. The results indicate a slight dependence of ignition time and combustion time on the flow rate of air into the reactor, showing a minimum between

Table 4
Composition of the fibreboard residues used

Fuel type	Moisture (wt% wB)	C	H	N	Volatiles (wt% dB)	Fixed carbon	Ash
Fibreboard waste	10.2	47	6	3.4	80.5	18.0	1.4

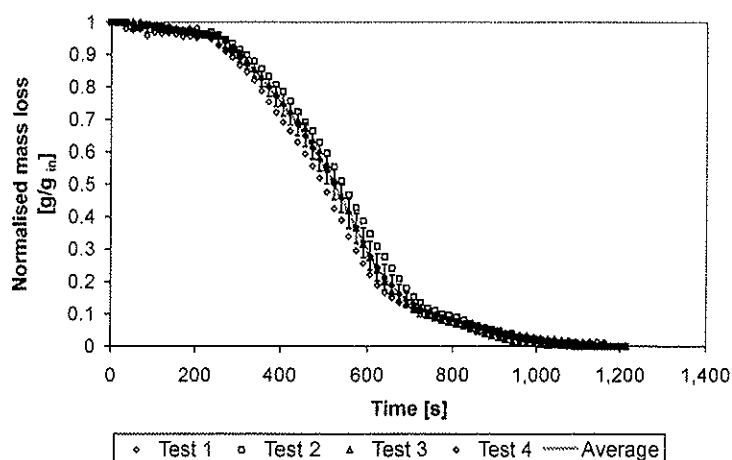


Fig. 13. Reproducibility of the normalised mass loss for the test runs at an air flow rate of $5.0 \times 10^{-4} \text{ m}^3/\text{s}$ into the reactor and an O_2 concentration of 21 vol%. The indicators mark the 95% confidence interval of the mean value of all test runs.

Table 5
Balances of H, C, and N using H₂O concentrations obtained by calculated calibration functions

Number	Window	Air flow rate (m ³ /s)	O ₂ concentration (vol%)	H-balance (mol/mol _{fuel})	C-balance (mol/mol _{fuel})	N-balance (mol/mol _{fuel})
1	ZnSe	3.33 × 10 ⁻⁴	21	0.70 ± 0.21	0.83 ± 0.17	0.40 ± 0.08
2	ZnSe	3.33 × 10 ⁻⁴	21	0.86 ± 0.26	1.07 ± 0.21	0.37 ± 0.07
3	Sapphire	3.33 × 10 ⁻⁴	21	0.82 ± 0.21	1.12 ± 0.17	–
Mean value		3.33 × 10 ⁻⁴	21	0.79 ± 0.08	1.01 ± 0.16	0.39 ± 0.02
4	ZnSe	4.17 × 10 ⁻⁴	21	1.03 ± 0.26	1.18 ± 0.18	0.60 ± 0.12
5	ZnSe	4.17 × 10 ⁻⁴	21	0.94 ± 0.24	1.06 ± 0.16	0.56 ± 0.11
6	Sapphire	4.17 × 10 ⁻⁴	21	0.82 ± 0.21	1.16 ± 0.17	–
7	Sapphire	4.17 × 10 ⁻⁴	21	0.97 ± 0.24	1.07 ± 0.16	–
Mean value		4.17 × 10 ⁻⁴	21	0.94 ± 0.09	1.12 ± 0.06	0.58 ± 0.03
8	ZnSe	5.00 × 10 ⁻⁴	21	0.67 ± 0.17	0.92 ± 0.14	0.46 ± 0.09
9	ZnSe	5.00 × 10 ⁻⁴	21	0.89 ± 0.22	1.13 ± 0.17	0.45 ± 0.09
10	ZnSe	5.00 × 10 ⁻⁴	21	0.90 ± 0.23	1.15 ± 0.17	0.39 ± 0.08
11	ZnSe	5.00 × 10 ⁻⁴	21	0.48 ± 0.12	0.63 ± 0.09	0.22 ± 0.04
Mean value		5.00 × 10 ⁻⁴	21	0.74 ± 0.20	0.96 ± 0.24	0.38 ± 0.11
12	ZnSe	5.83 × 10 ⁻⁴	21	0.86 ± 0.22	1.00 ± 0.15	0.36 ± 0.07
13	ZnSe	5.83 × 10 ⁻⁴	21	0.96 ± 0.24	1.17 ± 0.18	0.36 ± 0.07
14	Sapphire	5.83 × 10 ⁻⁴	21	0.69 ± 0.17	1.04 ± 0.16	±
Mean value		5.83 × 10 ⁻⁴	21	0.84 ± 0.14	1.07 ± 0.09	0.36 ± 0.07
15	ZnSe	6.67 × 10 ⁻⁴	21	0.71 ± 0.21	0.86 ± 0.17	0.25 ± 0.05
16	ZnSe	6.67 × 10 ⁻⁴	21	1.00 ± 0.30	1.13 ± 0.23	0.31 ± 0.06
17	ZnSe	6.67 × 10 ⁻⁴	21	0.91 ± 0.27	1.18 ± 0.24	0.28 ± 0.06
18	Sapphire	6.67 × 10 ⁻⁴	21	0.68 ± 0.17	0.97 ± 0.15	–
Mean value		6.67 × 10 ⁻⁴	21	0.83 ± 0.16	1.04 ± 0.15	0.28 ± 0.03
19	ZnSe	5.00 × 10 ⁻⁴	16	1.14 ± 0.34	0.85 ± 0.26	0.29 ± 0.09
20	ZnSe	5.00 × 10 ⁻⁴	16	1.00 ± 0.30	0.74 ± 0.22	0.24 ± 0.07
21	ZnSe	5.00 × 10 ⁻⁴	16	1.10 ± 0.33	0.82 ± 0.25	0.33 ± 0.10
Mean value		5.00 × 10 ⁻⁴	16	1.08 ± 0.32	0.80 ± 0.24	0.29 ± 0.09
22	ZnSe	5.00 × 10 ⁻⁴	13	1.08 ± 0.32	0.70 ± 0.21	0.32 ± 0.10
23	ZnSe	5.00 × 10 ⁻⁴	13	0.87 ± 0.26	0.63 ± 0.19	0.20 ± 0.06
24	Sapphire	5.00 × 10 ⁻⁴	13	0.97 ± 0.29	0.64 ± 0.19	–
25	ZnSe	5.00 × 10 ⁻⁴	13	1.14 ± 0.34	0.83 ± 0.25	0.27 ± 0.08
Mean value		5.00 × 10 ⁻⁴	13	1.02 ± 0.30	0.70 ± 0.21	0.26 ± 0.08

Note. H based on calculated calibration spectra, C, N based on measured calibration spectra; sapphire windows do not allow detection of NH₃ because the transparency of IR in the necessary wavelength is not given at higher temperatures; deviations ± show the estimated error of the FT-IR in situ absorption method [6,7].

4.67 × 10⁻⁴ m³/s and 5.83 × 10⁻⁴ m³/s. A reduction in [O₂] concentration from 21 to 13 vol% in the combustion air led to longer ignition times and longer combustion times, as well as lower peak temperatures in the reaction front and lower overall release rates of total fixed nitrogen [11].

NH₃ is the major nitrogen-containing species released from the fuel; it is mainly released during devolatilisation and during the transition to char burnout. During char burnout, N is mainly released as NO, but at a significantly lower level than NH₃ during devolatilisation. The release of HCN from the fuel was always almost negligible. The release of NO showed two significant peaks during all test runs: the first was observed shortly before the fuel ignited; the second was during char burnout. This behaviour of fibreboard has also been observed by others [5]. The

origin of the first peak, which makes a significant contribution to the NO released from the fuel, is probably the release of highly volatile N-containing additives to the fuel such as glue, binders, or coatings. Another possibility might be that the NO is caused by flaming conditions at the top of the bed of fuel, shortly before ignition. However, these flaming conditions were not detected by a sudden increase in any measured temperatures. The release of NO showed no significant dependence on flow rate or [O₂] at the inlet. This may also be caused by the low amount of char (15 wt% of the sample of 185 g) available for investigation. For better reproducibility of the release of NO and to deduce any trends in the release of NO, similar experiments are recommended using char only. Simulations of NO_x kinetics under the inlet conditions

used in this study have been published previously [11] using sensitivity analysis of the influence of varying inlet NO concentrations within the detected range of uncertainty. These results showed that the rate of the release of NO from the fuel had negligible influence on NO_x emissions over the range investigated [11,12].

For this reason the results presented will focus on the release of NH₃ during the drying and devolatilisation phases. Two types of parameter were investigated. Parameters remaining constant during a test run (SV_{inlet} , u_{RF}) were correlated with the overall rates of conversion of N in the fuel to NH₃, the only important nitrogenous species. Furthermore, pa-

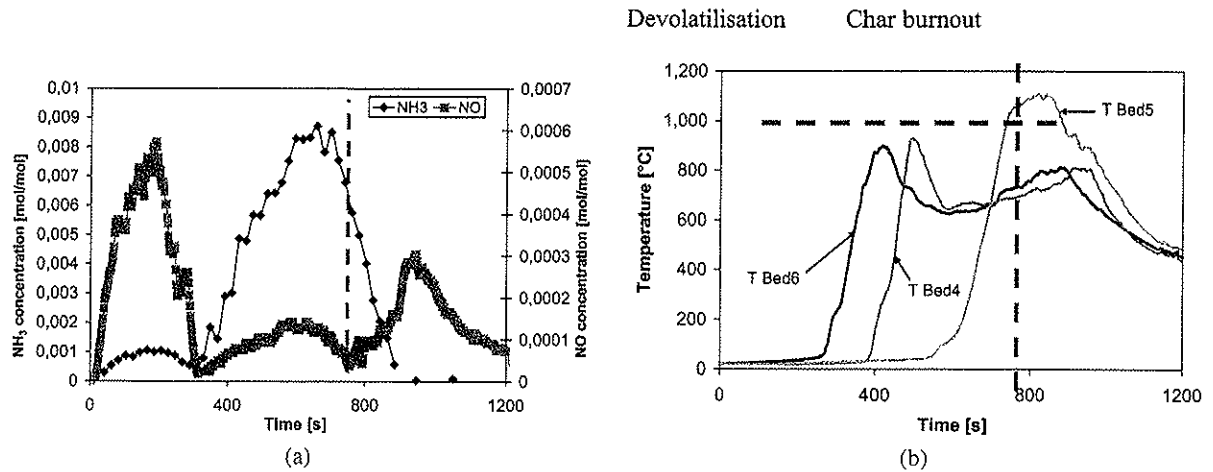


Fig. 14. Species concentrations and bed temperatures for a typical test run with fibreboard as fuel. (a) Release of NH₃ and NO; (b) temperature profile in the bed for a mean air flow of $5.0 \times 10^{-4} \text{ m}^3/\text{s}$ and an oxygen concentration of 21 vol%.

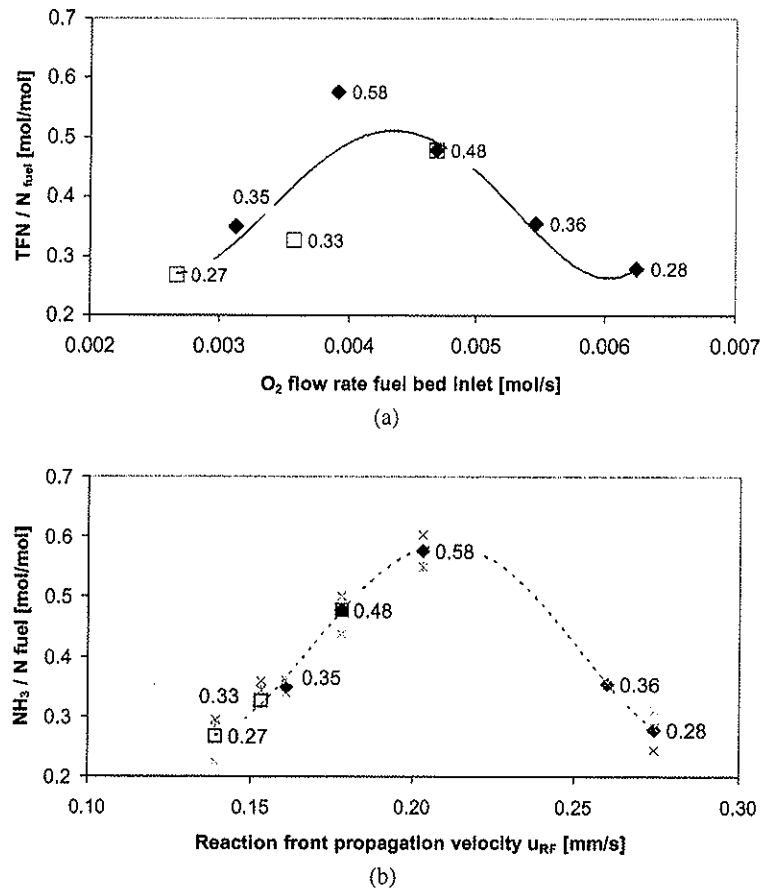


Fig. 15. Influence of molar flow rate of O₂ and propagation velocity of the reaction front on NH₃ conversion rates for the fuel fibreboard. Presented values are means of all test runs for each parameter; (◆) flow rate 3.3×10^{-4} to $6.67 \times 10^{-4} \text{ m}^3/\text{s}$, O₂ concentration 21 vol%; (□) flow rate $5.0 \times 10^{-4} \text{ m}^3/\text{s}$, O₂ concentration 13–21 vol%; (×) ... single test runs.

rameters varying during a test run (e.g., SV_{outlet} and $m/m_{\text{fuel_init}}$) were compared to instantaneous release rates of specific species (NH_3 , NO , CO , CO_2 , CH_4). This was done with the objective of finding parameters that allow inlet conditions to be described for CFD calculations of gas-phase combustion. Using these parameters, it should be possible to compute the release profiles of N species without any need to apply detailed N kinetics to the modelling of a fuel bed combusting on a grate. The advantage of this method should be that computationally intensive particle interactions in the fuel bed can be neglected for a description of N chemistry in the fuel bed and replaced by an experimentally developed empirical function. It should be sufficient to model the combustion specific parameter.

Investigation of the influence of SV_{inlet} and $[\text{O}_2]$ on overall rate of release of NH_3 shows that there is a maximum release at SV_{inlet} between 0.006 and 0.007 m/s (see Fig. 15). This value refers to a flow rate of the inlet gas between 4.17×10^{-4} and 5.0×10^{-4} m³/s. At higher flow rates the release rate decreases again. The reduction of $[\text{O}_2]$ from 21 to 13 vol% in the inlet gas stream at a constant flow rate de-

creases the rate of release of NH_3 and therefore also of total fixed nitrogen from the fuel (Fig. 15, Table 5). These effects may also be explained by the fact that the governing regime may change from reaction control to diffusion control at lower gas flow rates.

Reducing $[\text{O}_2]$ at a constant flow rate changes the stoichiometry in the fuel bed; hence SV_{inlet} is no longer a representative parameter. Combustion is delayed because $[\text{O}_2]$ and the temperature in the vicinity of the particle are decreasing. Taking the O_2 flow entering the fuel bed as a measure of the stoichiometry, no uniform trend in the rate of release of NH_3 could be detected (see Fig. 15a). It can be stated that the O_2 theoretically available is not the major parameter influencing the release of NH_3 from a fixed bed of fuel and therefore in itself is insufficient for a description of NH_3 release. Transport effects (cooling the particle, convective heat fluxes, temperature in the fuel bed, reaction front) must also be taken into consideration due to diffusion control.

The temperatures in the bed were found to depend on time. The peak temperatures of the thermocouples in the bed are characteristic of (and so are suitable for comparing) the conditions a particular experiment.

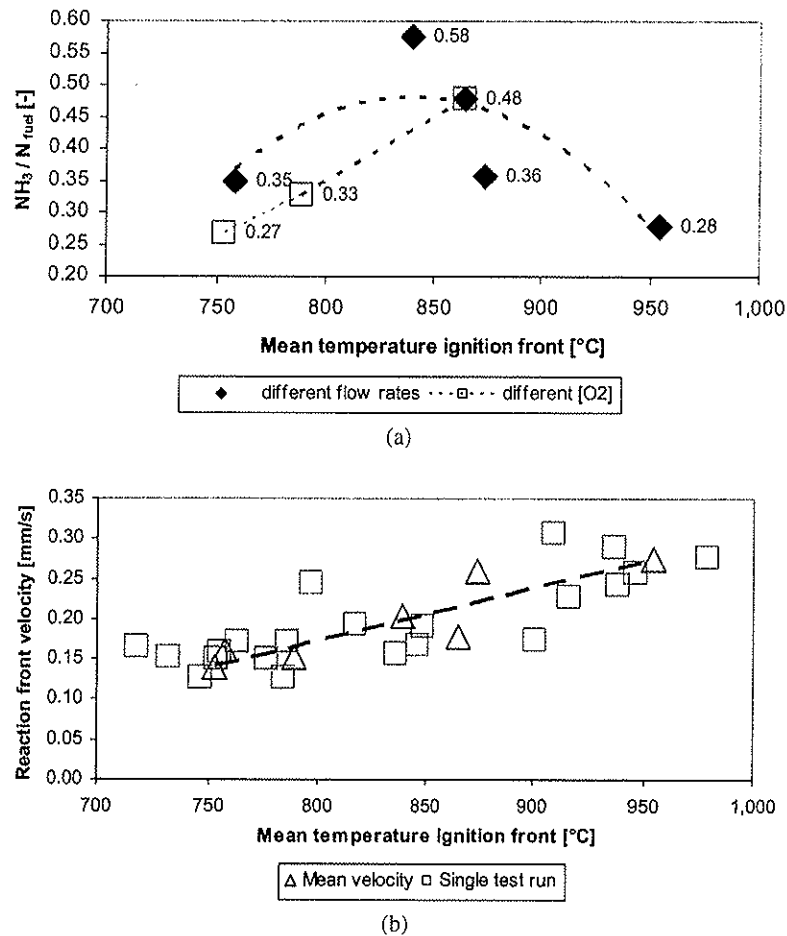


Fig. 16. NH_3 conversion as a function of the mean temperatures of the reaction front (a) and reaction front propagation velocity v_{RF} as a function of the mean temperature in the reaction front (b).

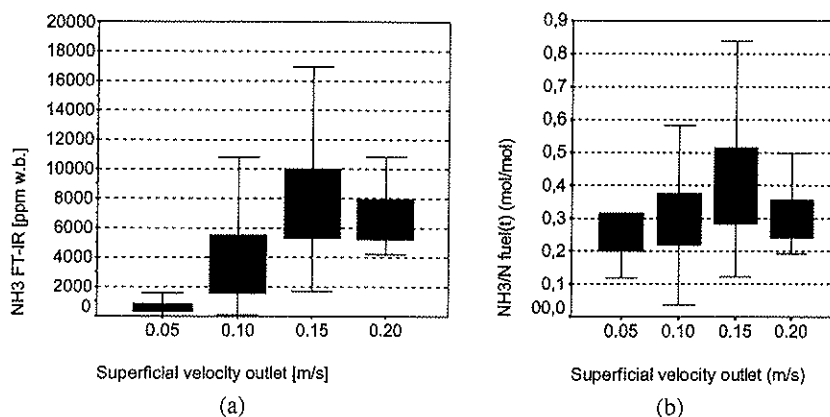


Fig. 17. Plots of (a) concentrations and (b) conversion rates of NH_3 against the instantaneous superficial velocity at the outlet of the bed.

These maximum temperatures can be interpreted as the temperatures in the reaction front. It can be assumed that the reaction front temperature remains constant while the front propagates downward. It is thus constant for a specific experiment and can be compared with the overall conversion rate of nitrogen. Although the propagation velocity of the reaction front rises with temperatures (see Fig. 16), the temperature in the reaction front alone does not characterise the release of NH_3 .

As already shown, both the flow rate of O_2 into the reactor and the temperature in the reaction front are not sufficient to describe the overall conversion rates for N during an experiment. A global parameter that implicitly describes the combustion process is necessary. Using the velocity of the reaction front, u_{RF} , as a parameter seems to be a good method of describing the release of N during the devolatilisation (Fig. 15b) and the transition stage to char burnout. During char burnout NH_3 is no longer released, but no significant dependence could be detected for NO.

For the simulation of N kinetics using CFD (computational fluid dynamics), the time-resolved release of nitrogen was also investigated. The time-dependent parameters SV_{outlet} , (Eq. (5)) and normalised mass loss (Eq. (6)) were investigated by test runs. Models for the description of these parameters are under development. Several models describing these parameters, as well as the propagation velocity of the reaction front have been published [1–4]. The stoichiometric ratio SR was also considered as a possible parameter, but investigations showed that it is less useful, so it will not be discussed further. A more detailed discussion can be found elsewhere [11].

The influence of SV_{outlet} is shown in Fig. 17a. It can be seen that a maximum $[\text{NH}_3]$ occurs at a SV_{outlet} of 0.15 m/s. As concentrations can only describe gas conditions, the total amount released was taken into consideration for the evaluation of the total release of N. The maximum rate of production of NH_3

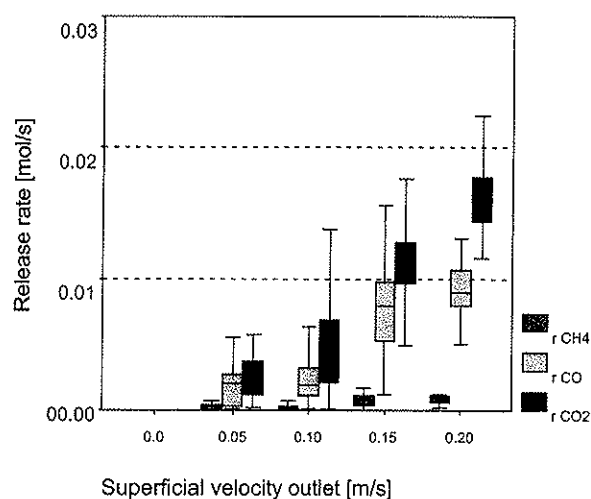


Fig. 18. Instantaneous release rates of the major species released from the fuel bed in relation to combustion specific parameters. All test runs with a constant O_2 concentration of 21 vol% were investigated.

(taking also the flow rate from the fuel bed into consideration) remains constant at $SV_{\text{outlet}} = 0.15$ m/s as shown in Fig. 17b. Thus SV_{outlet} provides good information about the combustion. Although the parameter provides no information about the stoichiometry, this parameter turned out to be adequate for describing the release, not only of NH_3 , but also of CO, CO_2 , and CH_4 (see Fig. 18).

Another possibility for describing the time-resolved influence on the release of N from the fuel is the normalised mass loss, which is easier to determine experimentally and theoretically on a grate. Also the mass loss can easily be determined on a grate by investigating the ash and moisture contents of samples taken from various positions of the grate. The profiles of the release of N can also be determined using empirically fitted functions and adapted to experimental results. In this case a simple description of the mass

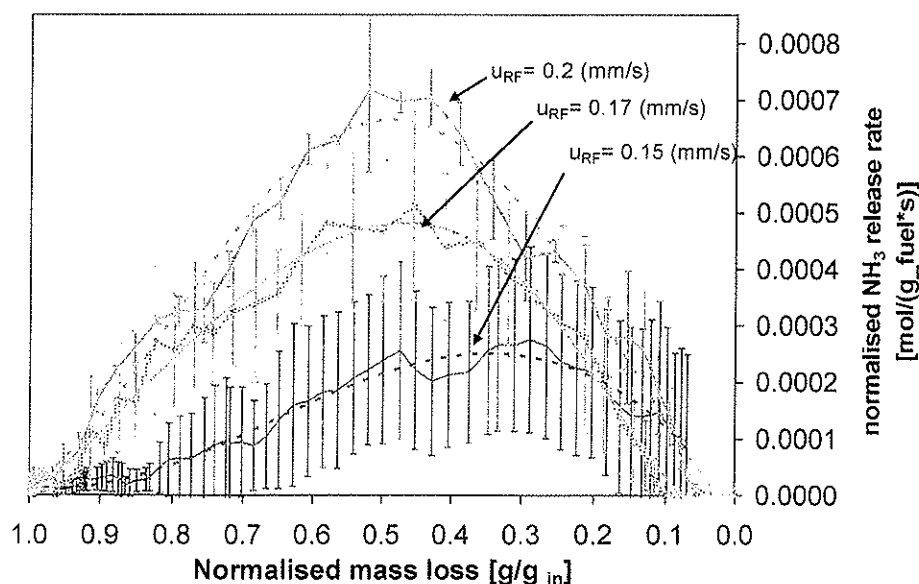


Fig. 19. NH_3 release rates as a function of the mass degradation for various combustion conditions indicated by reaction front propagation velocities u_{RF} in the fuel bed. The release rate refers to an initial fuel amount of 187 g, a nitrogen content of 3.5% d.b., and a moisture of 10% w.b.; if not mentioned, the O_2 concentration in the gas flow is 21 vol%; the occurring reaction front propagation velocities are according to Table 6.

Table 6

Mean concentrations of the major species in the gas phase during the drying and gasification phase within the test runs

Parameter	Unit	Test 1	Test 2	Test 3	Test 4	Test 5	Test 6	Test 7
O_2 concentration	vol%	21.0	21.0	21.0	21.0	21.0	16.0	13.0
Gas flow	m^3/s	0.0003	0.0004	0.0005	0.0006	0.0007	0.0005	0.0005
SV_{inlet}	m/s	0.050	0.06	0.07	0.08	0.09	0.07	0.07
u_{RF}	mm/s	0.160	0.20	0.17	0.26	0.27	0.15	0.14
$\text{H}_2\text{O}_{\text{FTIR}}$	[mol/mol]	0.23	0.25	0.18	0.20	0.20	0.14	0.11
$\text{CO}_2_{\text{FTIR}}$	[mol/mol]	0.17	0.18	0.18	0.18	0.17	0.13	0.11
CO_{FTIR}	[mol/mol]	0.09	0.11	0.09	0.10	0.10	0.07	0.06
$\text{CH}_4_{\text{FTIR}}$	[mol/mol]	0.011	0.012	0.10	0.010	0.011	0.008	0.007
$\text{NH}_3_{\text{FTIR}}$	[mol/mol]	0.003	0.007	0.007	0.006	0.005	0.006	0.006
NO_{OLD}	[mol/mol]	0.0001	0.0003	0.0002	0.0001	0.0001	0.0003	0.0004
HCN wet chemical	[mol/mol]	0.000001	0.000001	0.000002	0.000003	0.000001	0.000001	0.000000
N_2 (balance)	[mol/mol]	0.49	0.44	0.53	0.50	0.52	0.65	0.70
Total	[mol/mol]	1.00	1.00	1.00	1.00	1.00	1.00	1.00

Note. FT-IR measured with in situ absorption spectroscopy; CLD measured by extractive techniques using chemoluminescence detection (ECO-Physics 740 ht).

loss as a function of the distance from the fuel entry at the grate and the information of flow conditions along the grate would be necessary. For different boundary conditions (gas flow, O_2 concentration, u_{RF}), the release of NH_3 and the release rates of other major gaseous species can be described by a function of the normalised mass degradation (see Fig. 19 and Table 6), which itself is a function of time (fixed bed combustion model) or distance (experimentally derived). This approach is of special interest for defining release profiles of N from a fixed bed of fuel as a basis for subsequent CFD simulation of gas-phase combustion.

5. Conclusions

A laboratory-scale reactor was used to measure $[\text{NH}_3]$ using FT-IR in situ absorption spectroscopy during the release of gaseous compounds from fixed bed burning fibreboard residues. Spectra of NH_3 were measured at temperatures between 300 and 800 °C. A comparison with spectra calculated using the spectral database HITRAN showed on the one hand large deviations in a spectral region between 935 and 955 cm^{-1} , but satisfactory agreement in the other spectral regions on the other hand. The deviations can be explained by the fact that HITRAN was orig-

inally designed for ambient temperature applications. At high temperatures, lines may be missing in the HITRAN database or may have been calculated wrongly [8]. Experimental verification of high-temperature calculations was thus necessary, so the release of H, C, and N from the fuel was measured for different flow rates of air and [O₂] contents.

The effects of various parameters on the release of nitrogenous species during combustion were investigated using a discontinuously operated pot furnace, and in particular investigating a propagating reaction front. In fact, of those parameters remaining constant during an experiment, the propagation velocity of the reaction front turned out to be the parameter most suitable for describing the overall conversion of nitrogen-containing species during devolatilisation. NH₃ is the major nitrogenous species released, while significantly lower levels of NO and almost negligible amounts of HCN were measured. For a description of N release during char burnout, test runs with charcoal only are recommended. The parameters investigated (SV_{inlet} , SV_{outlet} , u_{RF}) are suitable for describing the release of nitrogenous compounds from the fuel, because they implicitly describe the combustion behaviour.

Of the time-dependent parameters investigated, SV_{outlet} and the normalised mass loss provided a good description of the release of NH₃, the major N-containing species. The normalised mass loss has the advantage that it can be calculated from theoretical models of combustion in a fixed bed as well as investigated experimentally. The methodology developed allows experimental investigation of the release profiles of nitrogenous species, as a function of either time or distance along a grate. These profiles may serve as reliable input profiles for CFD simulations of gas-phase combustion, which is becoming of increasing importance in the design of furnaces and boilers.

Acknowledgments

This work was supported by the Austrian Industrial Research Promotion Fund (FFF), O.Oe.Energies-

parverband, and the biomass furnace and boiler manufacturer MAWERA in Hard/Austria.

References

- [1] R. Gort, PhD thesis, Universiteit Twente, Enschede, CIP-Gegevens Koninklijke Bibliotheek, Den Haag, Netherlands, 1995.
- [2] B. Leckner, H. Thunman, *Fuel* 80 (2001) 473–481.
- [3] J.J. Saastamoinen, R. Taipale, M. Horttanainen, P. Sarkoma, *Combust. Flame* 123 (2000) 214–226.
- [4] R.P. Van der Lans, L.T. Pedersen, A. Jensen, P. Glarborg, K. Dam-Johansen, in: Addendum Proceedings of the 4th Biomass Conference of the Americas, September 1999, Oakland, CA, USA, 1999, Oxford, UK.
- [5] R. Keller, Forschungsbericht, Nr. 18, Laboratorium für Energiesysteme, ETH, Zürich, Schweiz, 1994.
- [6] T. Fleckl, H. Jäger, I. Obernberger, in: Proceedings of the 5th European Conference on Industrial Furnaces and Boilers, April 2000, Porto, Portugal, INFUB, Rio Tinto, Portugal, 2000.
- [7] T. Fleckl, H. Jäger, I. Obernberger, *J. Phys. D: Appl. Phys.* 35 (2001) 3138–3144, ISSN 00223727.
- [8] L.S. Rothman, C.P. Rinsland, A. Goldman, S.T. Massie, D.P. Edwards, J.-M. Flaud, A. Perrin, C. Camy-Peret, V. Dana, J.-Y. Mandin, J. Schroeder, A. Mccann, R.R. Gamache, R.B. Watson, K. Yoshino, K.V. Chance, K.W. Jucks, L.R. Brown, V. Nemchinov, P. Varanasi, *The HITRAN Molecular Spectroscopic Database and HAWKS*, 1996 ed., Manual, 1996.
- [9] L.S. Clesceri, A.E. Greenberg, A.D. Eaton, *Standard Methods for the Examination of Water and Wastewater*, twentieth ed., 1998.
- [10] A. Weissinger, T. Fleckl, I. Obernberger, in: Proceedings of the 1st World Conference on Biomass for Energy and Industry June 2000, vol. II, 2000, pp. 1729–1733.
- [11] A. Weissinger, Dissertation, Institut für Grundlagen der Verfahrenstechnik und Anlagentechnik, Technische Universität Graz, 2002.
- [12] A. Weissinger, I. Obernberger, R. Scharler, in: Proceedings of the 1st World Conference on Biomass for Energy and Industry June 2000, vol. II, James&James Ltd, London, UK, 2000, pp. 1935–1939.